Supplementary materials for

Eddy covariance fluxes of CO_2, CH_4 and N_2O on a drained peatland forest after clearcutting

by Tikkasalo et al.

Contents:

Table S1. Comparison of model performance measured with both leave-one-out cross-validation (LOO) and the adjusted coefficient of determination (R^2_{adj}). The model exhibiting the most favorable characteristics was selected for subsequent analysis and is presented in bold for both the CH_4 and N_2O fluxes.

Model	Number of parameters	LOO	R^2_{adj}
CH_4			
Simple	2	2446.0	0.407
Full ST3	9	2584.3	0.438
Full ST4	11	2617.6	0.446
Full ST5	13	2589.6	0.440
Full ST6	**15**	**2634.5**	**0.450**
Full ST9	21	2634.0	0.450
N_2O			
Simple	2	-3751.5	0.221
Full ST3	9	-3084.6	0.400
Full ST4	11	-3083.3	0.400
Full ST5	13	-2763.2	0.471
Full ST6	15	-2752.4	0.472
Full ST9	**21**	**-2704.2**	**0.482**
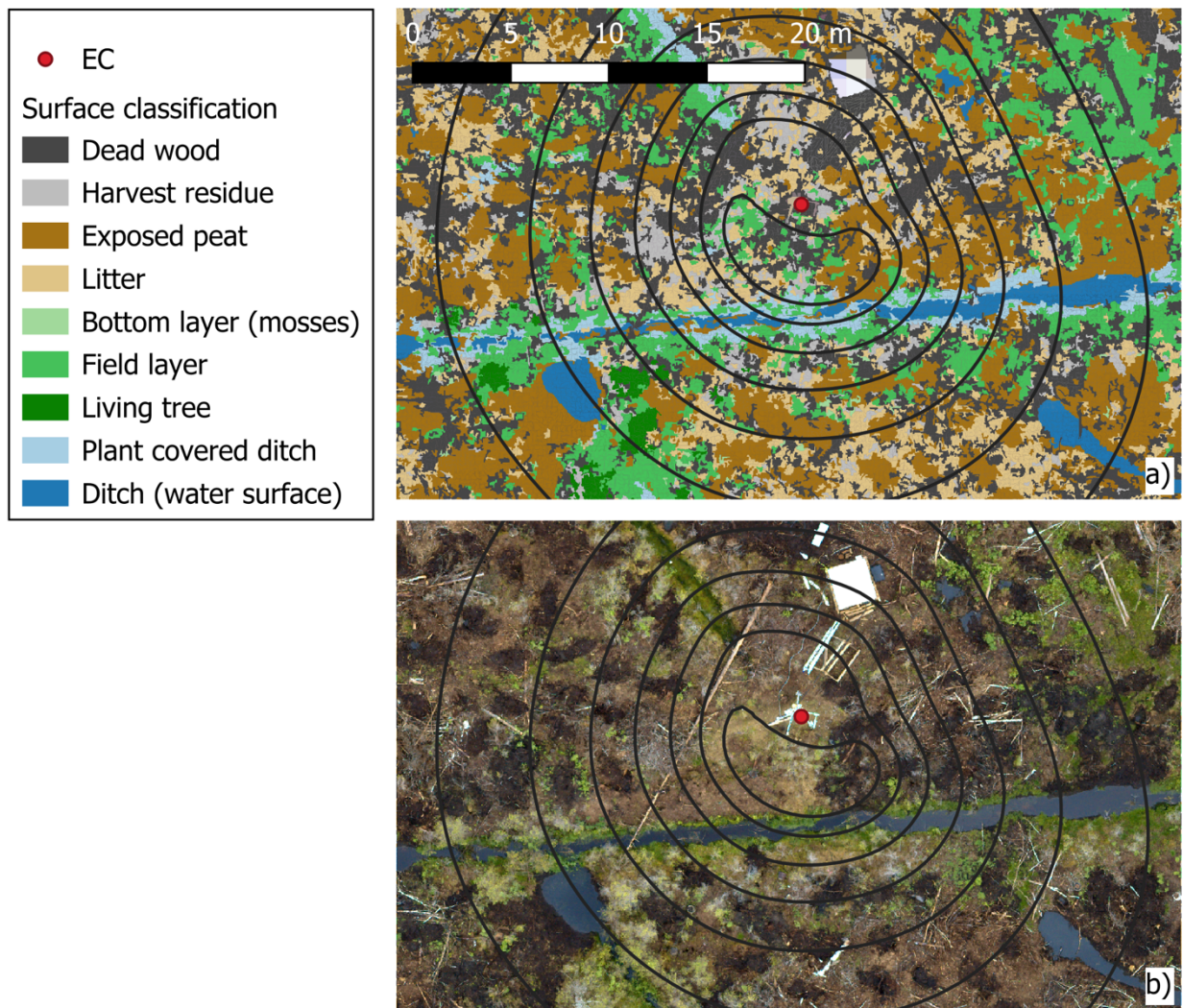
Figure S1. Close-up of surface-type classification (a) and aerial view (b) around the eddy covariance tower.
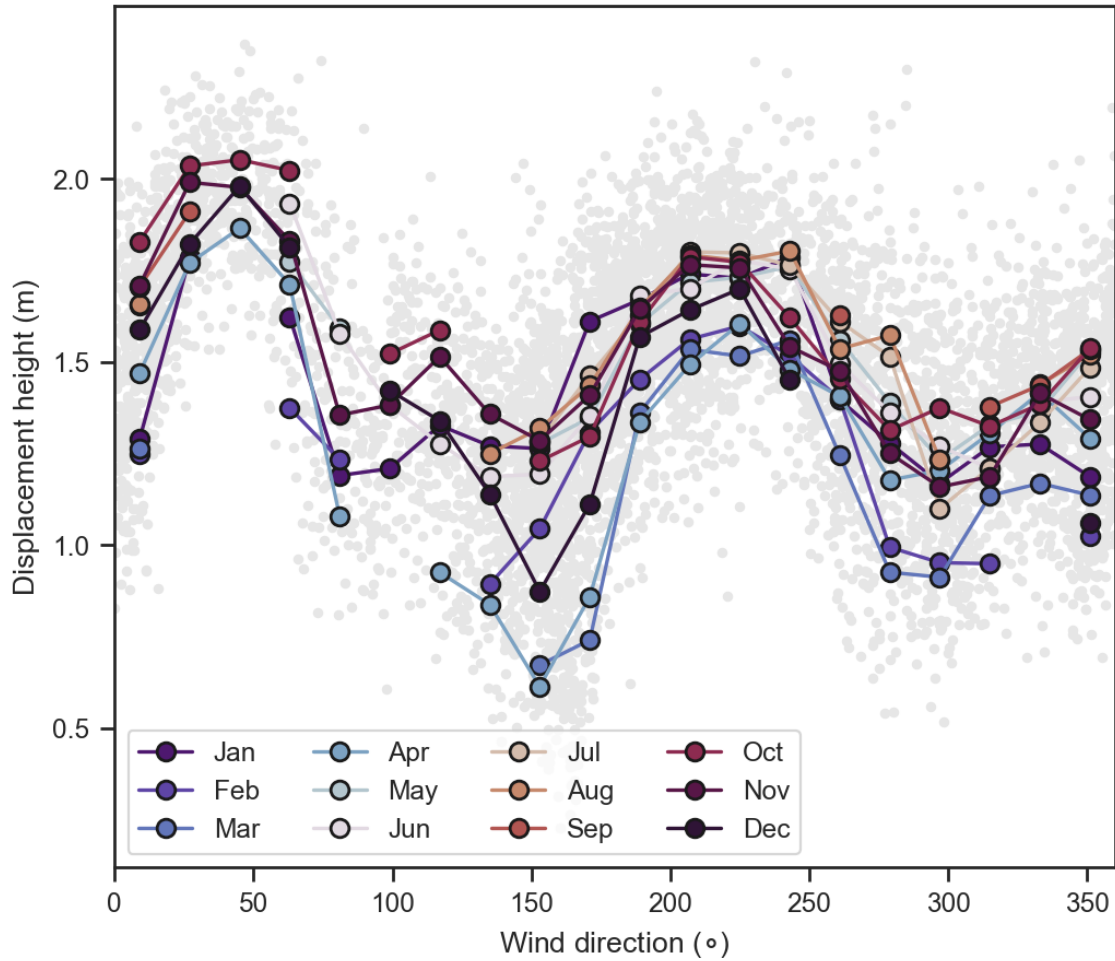
Figure S2. Displacement height at different wind directions. Grey markers shows the estimated displacement height (see Sect 2.4 in the main text) at different wind directions. Solid lines with circle markers shows the 30-day displacement height bins for each month that were used in the footprint calculations.
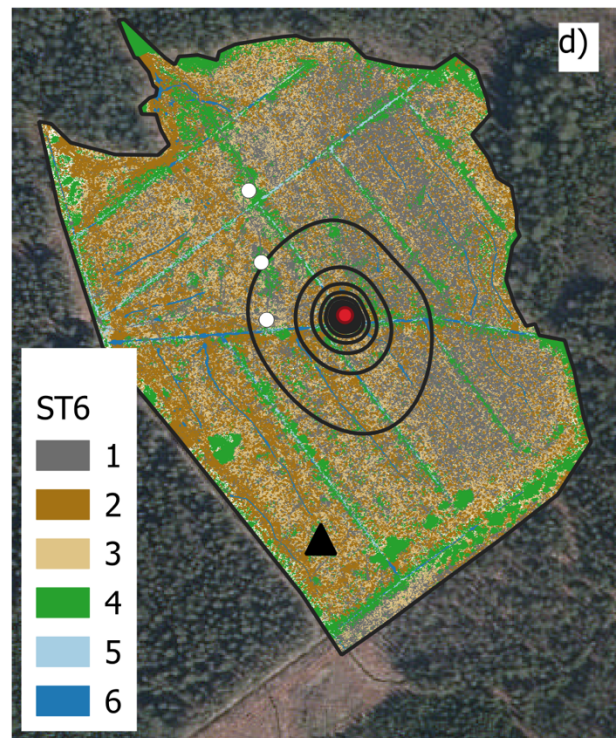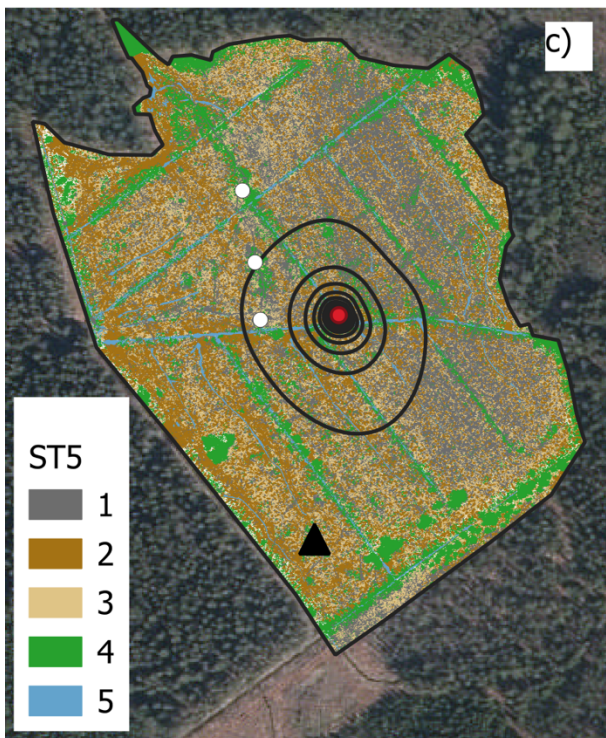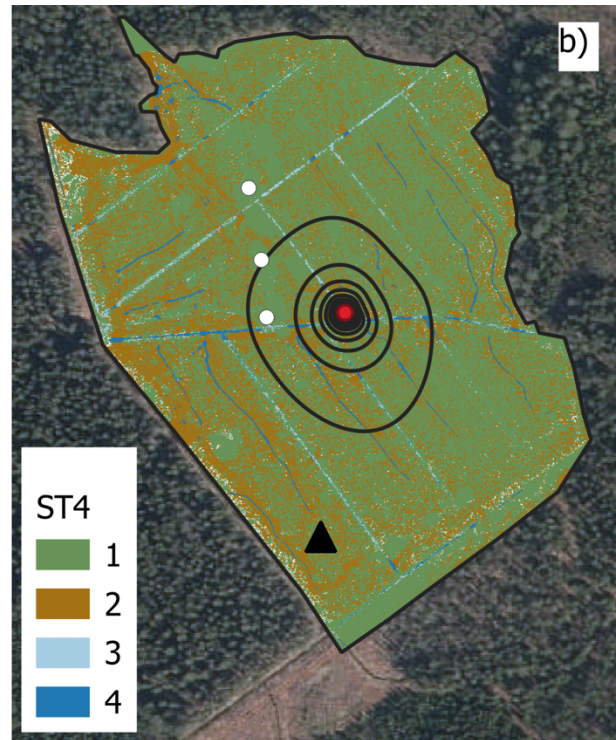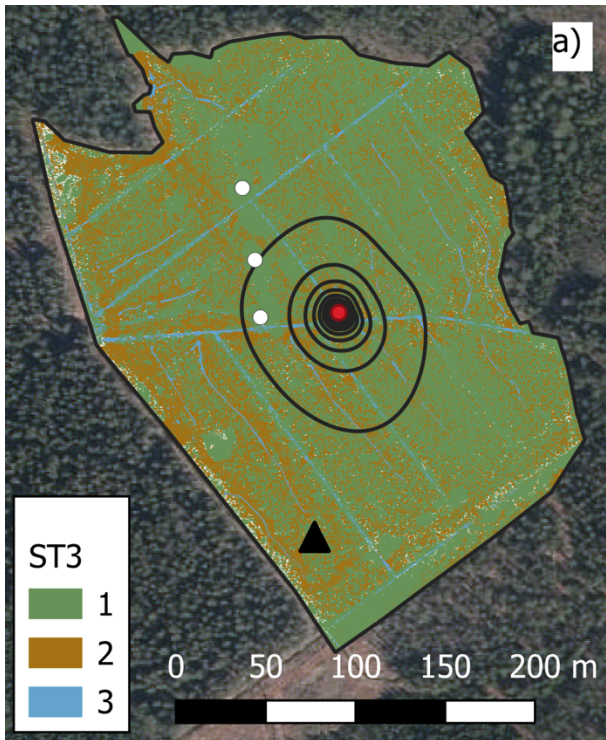
Figure S3: Surface-type classification for the clearcut area. The surface-type classification is shown for ST3 (a), ST4 (b), ST5(c) and ST6 (d). The surface-type combinations can be found from Table 3 in the main text. The background aerial photo in a-d is acquired from the National Land Survey of Finland Topographic Database (distributed with CC-BY 4.0 license, retrieved 06/2024).
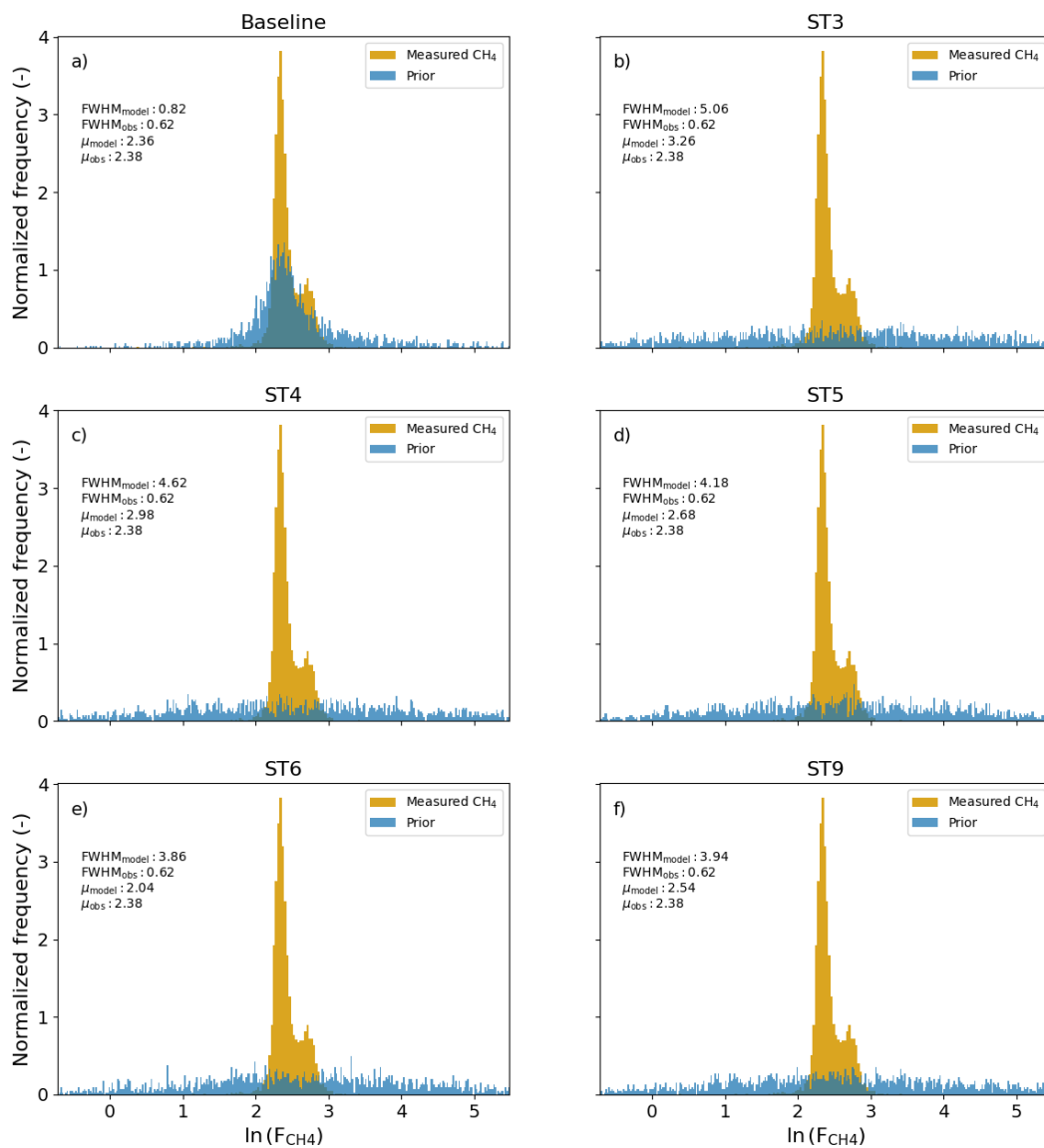
Figure S4. Prior predictive distribution and measured distribution of CH4 at the Ränskälänkorpi study site. Different subfigures are for different models described in the main text. Each subfigure shows the full width at half maximum (FWHM) and mean value of the prior predictive and measured distribution.
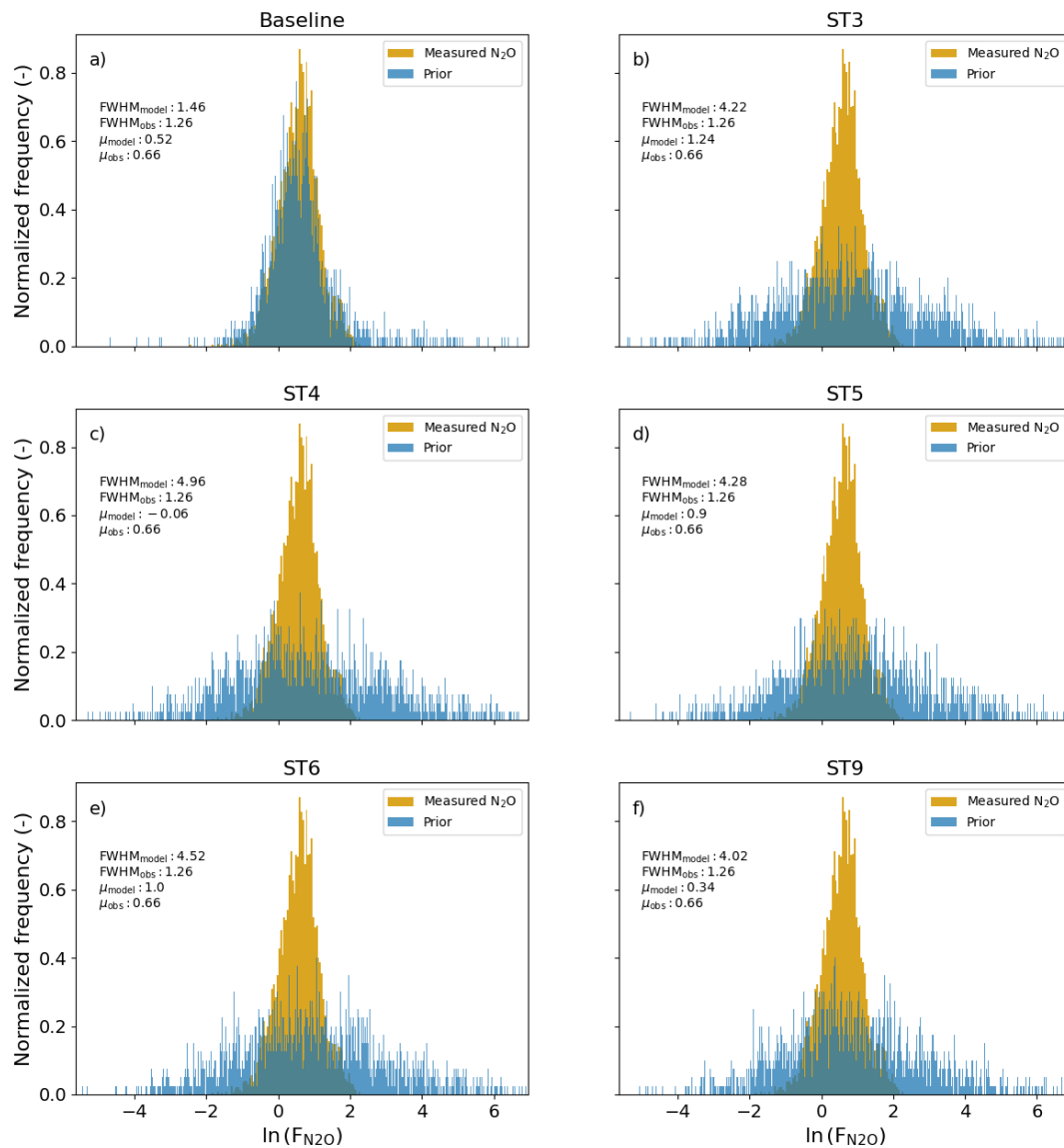
Figure S5. Prior predictive distribution and measured distribution of N₂O at the Ränskälänkorpi study site. Different subfigures are for different models described in the main text. Each subfigure shows the full width at half maximum (FWHM) and mean value of the prior predictive and measured distribution.
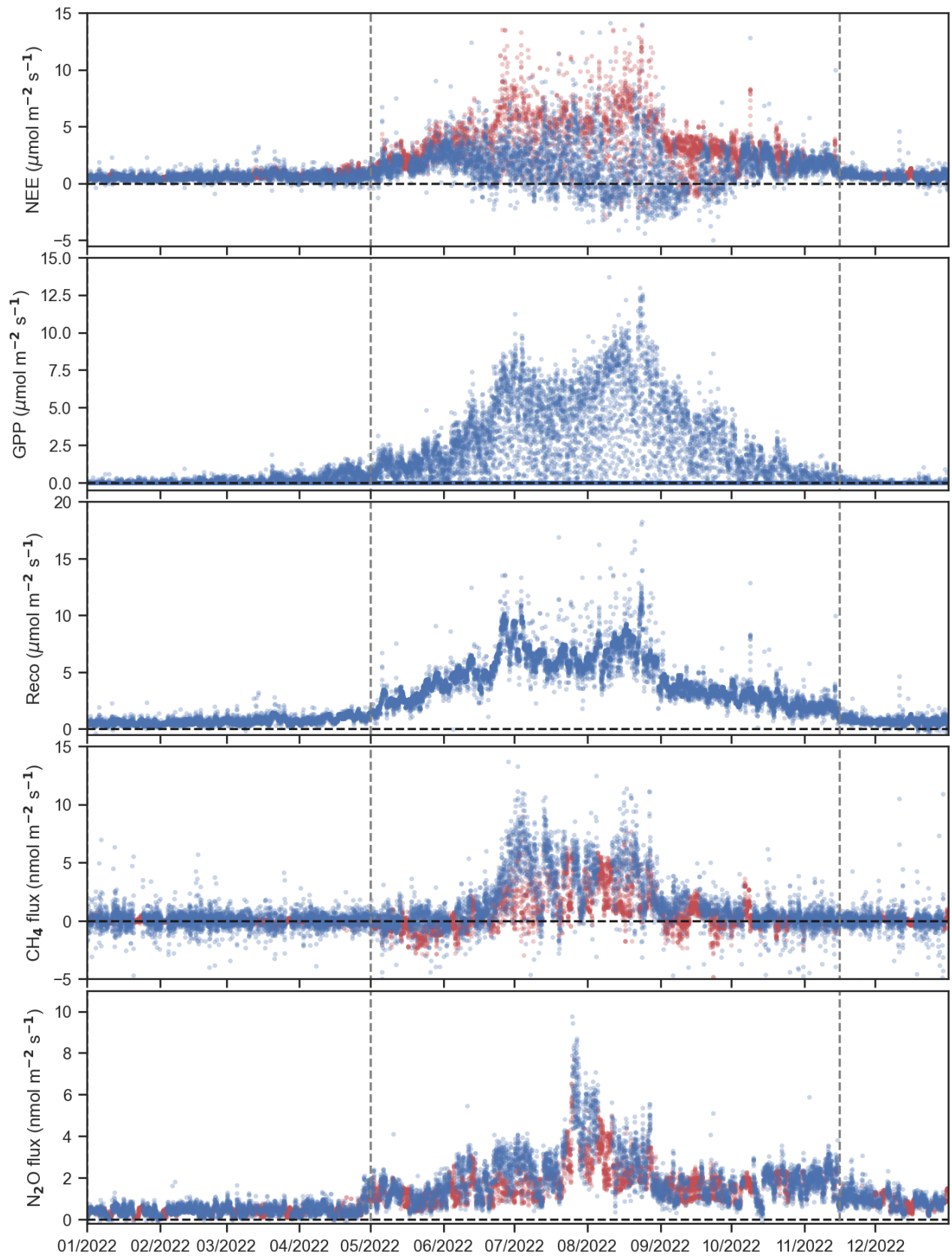
Figure S6. Time series of 30 min fluxes during the year 2022. Red symbols show gapfilled values and blue show measured values.
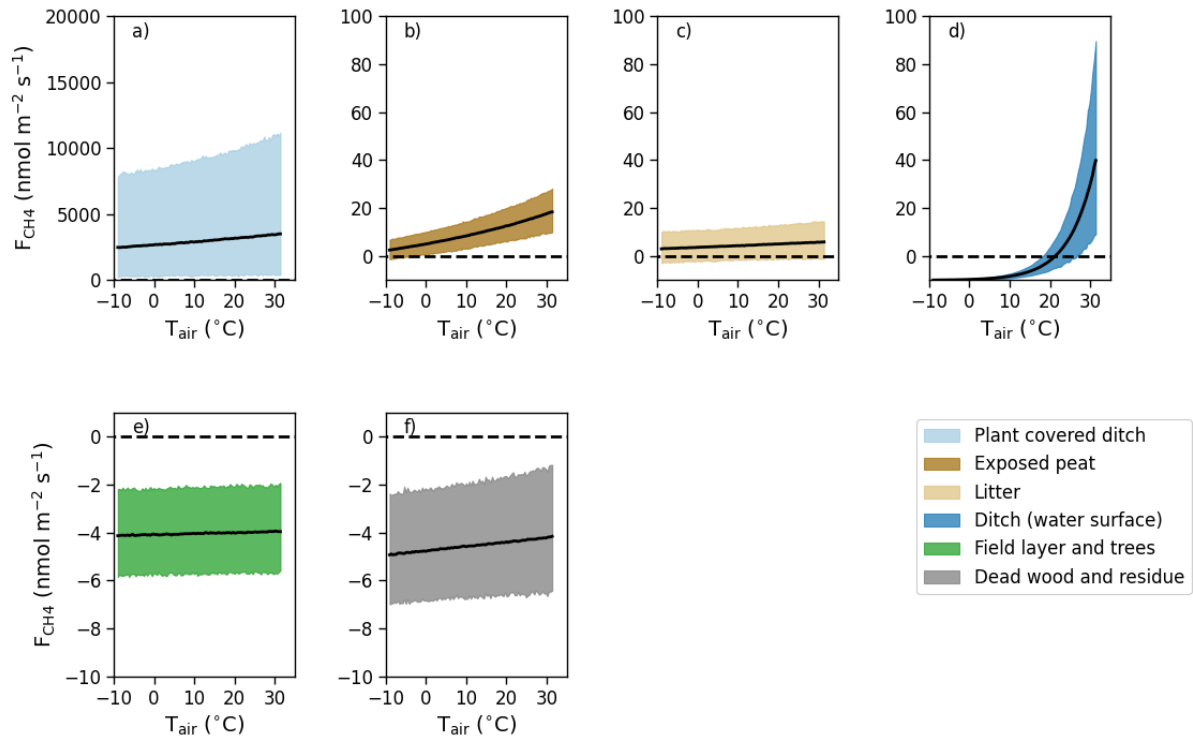
Figure S7. Temperature response of each surface type for the best CH₄ model. The estimate is calculated for each temperature and surface type by setting the surface type contribution to unity ($\varphi_{i,j}=1$ in Eq. 4 in the main text) and calculating the estimate 8000 times using the parameter sets sampled in the MCMC step. The shaded area shows the 95th highest density interval and the black line the mean estimate. The air temperature values were set by dividing the interval between maximum and minimum measured air temperature into 101 values.
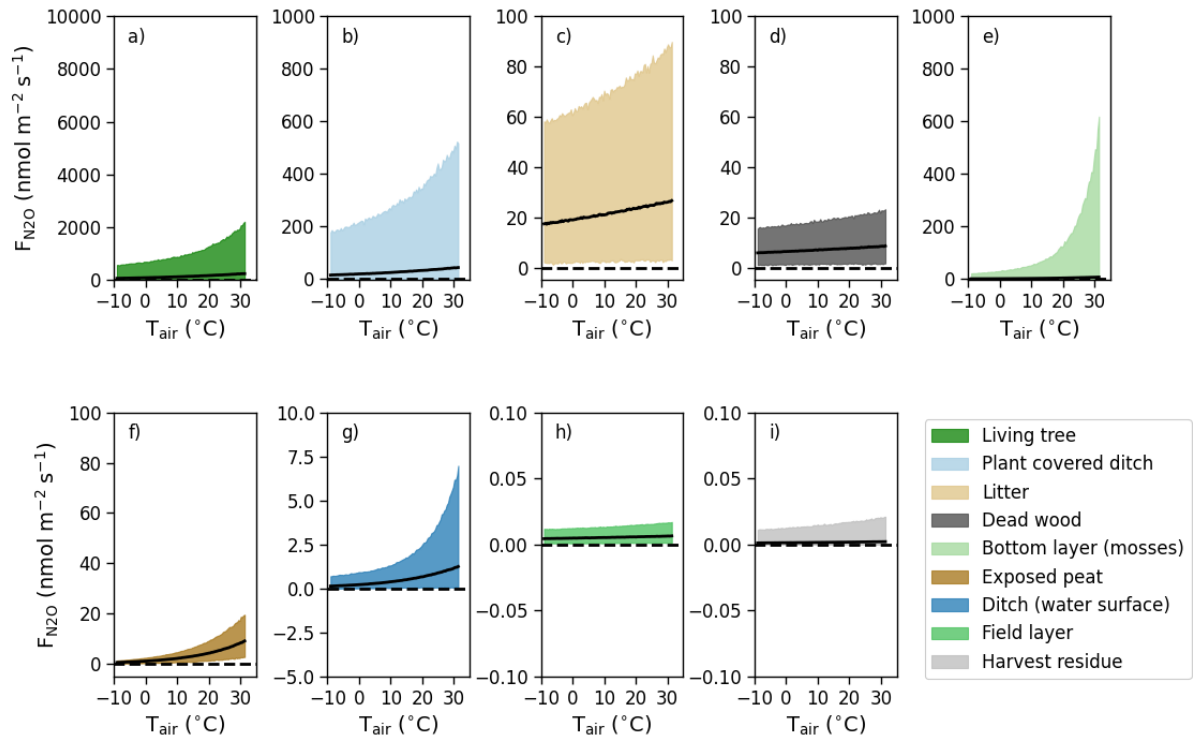
Figure S8. Temperature response of each surface type for the best N₂O model. The estimate is calculated for each temperature and surface type by setting the surface type contribution to unity ($\varphi_{i,j}=1$ in Eq. 4 in the main text) and calculating the estimate 8000 times using the parameter sets sampled in the MCMC step. The shaded area shows the 95th highest density interval and the black line the mean estimate. The air temperature values were set by dividing the interval between maximum and minimum measured air temperature into 101 values.
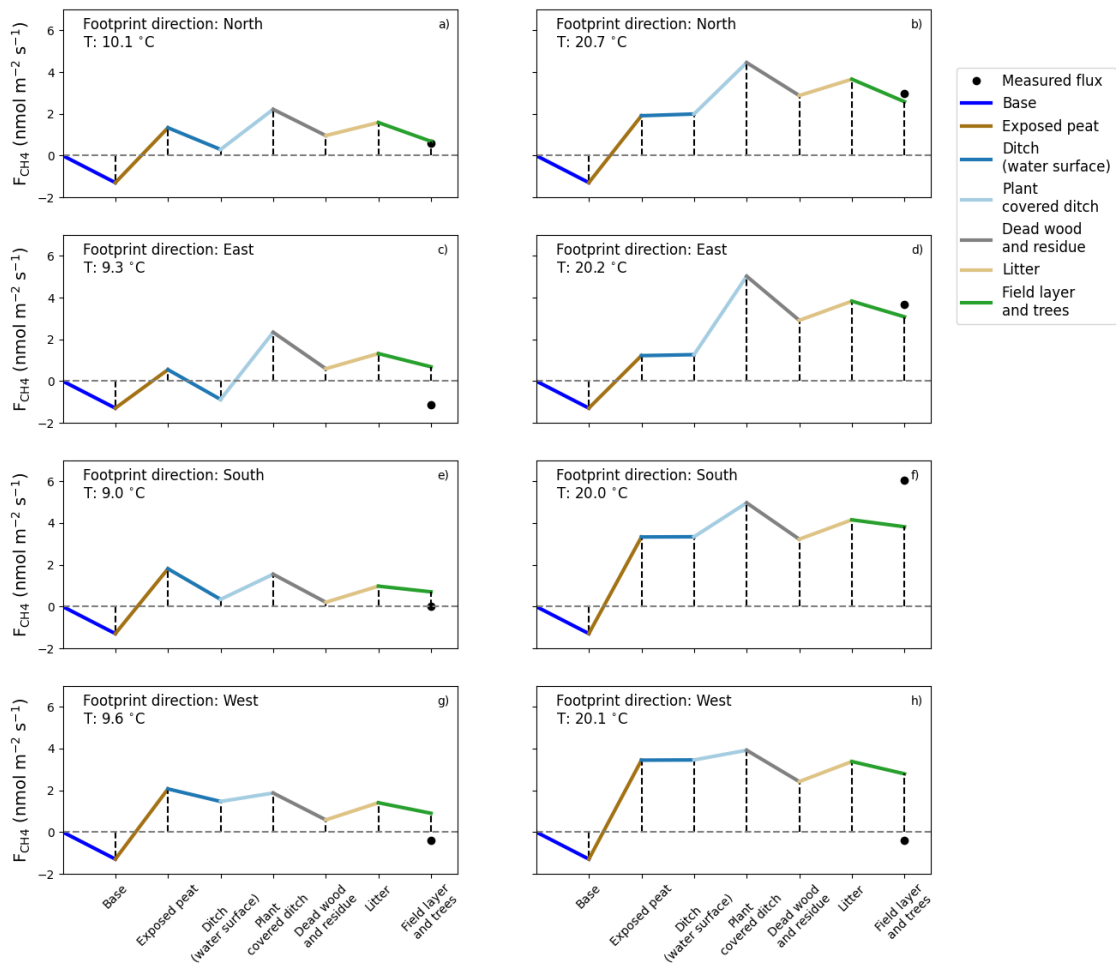
Figure S9. Contribution of each surface type to the estimated flux value in the CH₄ model. Different subfigures show different footprint directions in the clearcut (see Fig. 1 in the main text) and the left column is for the measurement whose air temperature is closest to 283.15 K (=10°C) and right for the air temperature 293.15 K (=20°C). In each subfigure, surface types are added to the model from left to right. Base model is the baseline model as defined by Eq. (3) in the main text. Black circle shows the value of the measured flux and the final model estimate is found on the last surface type (Field layer and trees) on the horizontal axis.
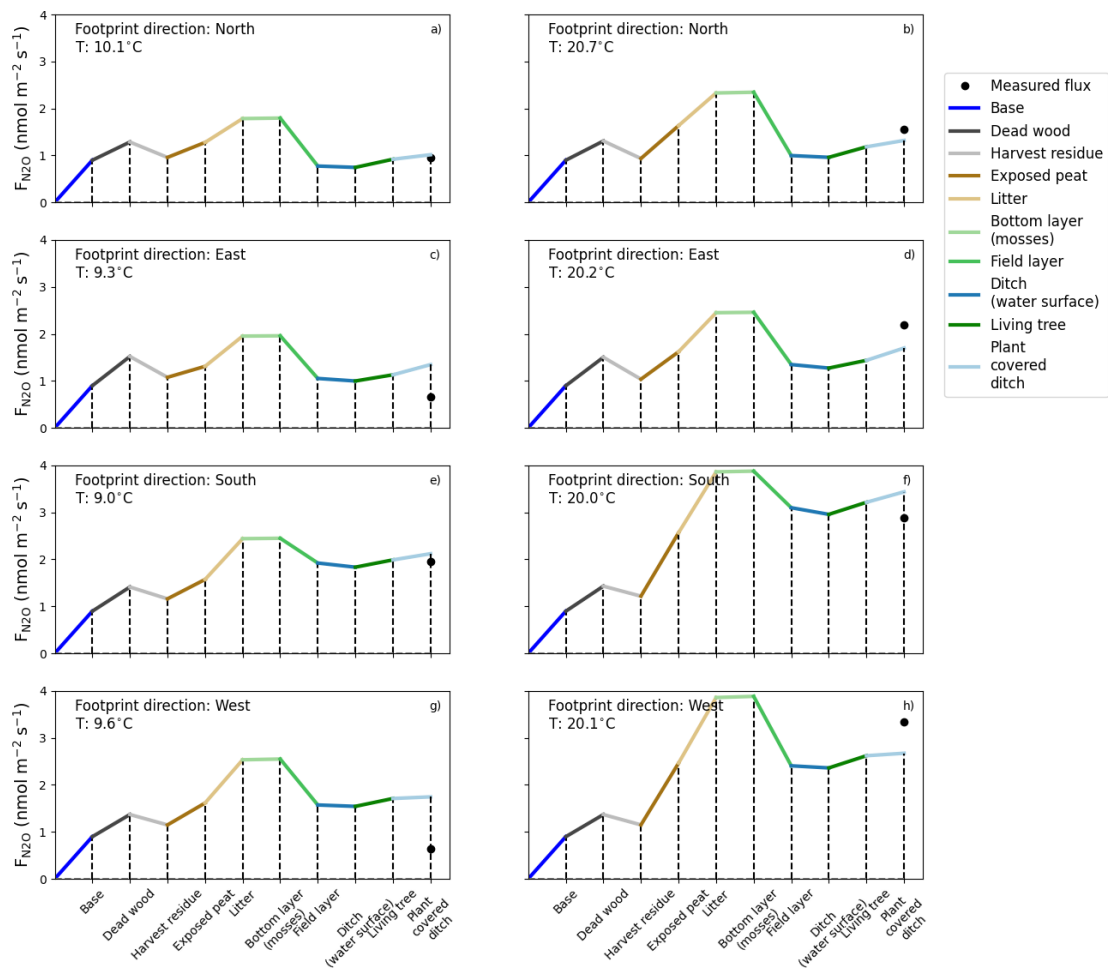
Figure S10. Contribution of each surface type to the estimated flux value in the N₂O model. Different subfigures show different footprint directions in the clearcut (see Fig. 1 in the main text) and the left column is for the measurement whose air temperature is closest to 283.15 K (=10°𝐶) and right for the air temperature 293.15 K (=20°𝐶). In each subfigure, surface types are added to the model from left to right. Base model is the baseline model as defined by Eq. (3) in the main text. Black circle shows the value of the measured flux and the final model estimate is found on the last surface type (Plant covered ditch) on the horizontal axis.
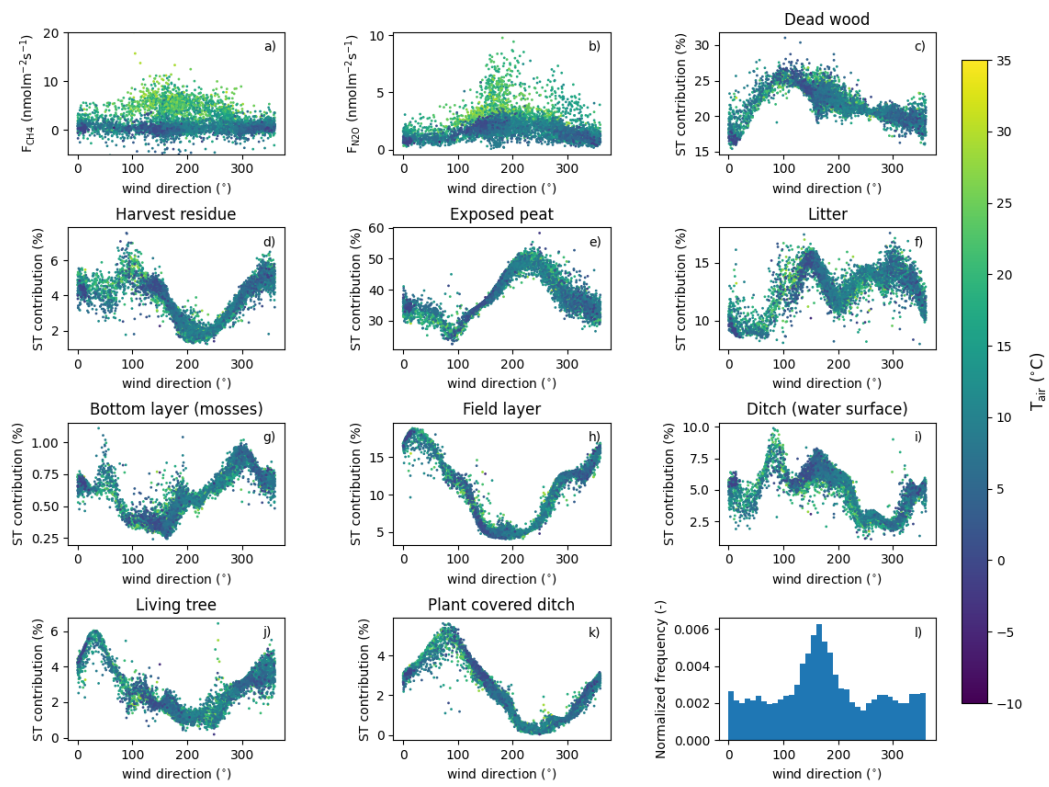
Figure S11. Analysis of wind direction dependencies. Wind direction dependency of CH_4 (a) and N_2O (b) fluxes, each surface-type contribution inside the eddy covariance footprint (c-k), and distribution of footprint wind directions (k). Color in panels a-k shows the air temperature.